



Iodine budget in surface waters from Atacama: Natural and anthropogenic iodine sources revealed by halogen geochemistry and iodine-129 isotopes



Fernanda Álvarez ^{a, b, c, *}, Martin Reich ^{a, b}, Glen Snyder ^d, Alida Pérez-Fodich ^{b, e}, Yasuyuki Muramatsu ^f, Linda Daniele ^{a, b}, Udo Fehn ^g

^a Department of Geology, FCFM, Universidad de Chile, Santiago, Chile

^b Andean Geothermal Center of Excellence (CEGA), FCFM, Universidad de Chile, Santiago, Chile

^c Departamento de Ciencias de la Tierra, Universidad de Concepción, Casilla 160-C, Concepción, Chile

^d Gas Hydrate Research Laboratory, Meiji University Global Front, Tokyo 101-8301, Japan

^e Department of Earth and Atmospheric Sciences, Cornell University, Ithaca, NY 14853, USA

^f Department of Chemistry, Gakushuin University, Tokyo 113-0033, Japan

^g Department of Earth and Environmental Sciences, University of Rochester, Rochester, NY 14627, USA

ARTICLE INFO

Article history:

Received 17 November 2015

Received in revised form

24 March 2016

Accepted 25 March 2016

Available online 28 March 2016

Keywords:

Iodine

natural waters

iodine isotopic ratios

anthropogenic sources

ABSTRACT

Iodine enrichment in the Atacama Desert of northern Chile is widespread and varies significantly between reservoirs, including nitrate-rich “caliche” soils, supergene Cu deposits and marine sedimentary rocks. Recent studies have suggested that groundwater has played a key role in the remobilization, transport and deposition of iodine in Atacama over scales of millions-of-years. However, and considering that natural waters are also anomalously enriched in iodine in the region, the relative source contributions of iodine in the waters and its extent of mixing remain unconstrained. In this study we provide new halogen data and isotopic ratios of iodine ($^{129}\text{I}/\text{I}$) in shallow seawater, rivers, salt lakes, cold and thermal spring water, rainwater and groundwater that help to constrain the relative influence of meteoric, marine and crustal sources in the Atacama waters. Iodine concentrations in surface and ground waters range between 0.35 μM and 26 μM in the Tarapacá region and between 0.25 μM and 48 μM in the Antofagasta region, and show strong enrichment when compared with seawater concentrations ($\text{I} = \sim 0.4 \mu\text{M}$). In contrast, no bromine enrichment is detected (1.3–45.7 μM for Tarapacá and 1.7–87.4 μM for Antofagasta) relative to seawater ($\text{Br} = \sim 600 \mu\text{M}$). These data, coupled to the high I/Cl and low Br/Cl ratios are indicative of an organic-rich sedimentary source (related with an “initial” fluid) that interacted with meteoric water to produce a mixed fluid, and preclude an exclusively seawater origin for iodine in Atacama natural waters. Iodine isotopic ratios ($^{129}\text{I}/\text{I}$) are consistent with halogen chemistry and confirm that most of the iodine present in natural waters derives from a deep initial fluid source (*i.e.*, groundwater which has interacted with Jurassic marine basement), with variable influence of at least one atmospheric or meteoric source. Samples with the lowest isotopic ratios ($^{129}\text{I}/\text{I}$ from ~ 215 to $\sim 1000 \times 10^{-15}$) strongly suggest mixing between the groundwater and iodine storage in organic-rich rocks (with variable influence of volcanic fluids) and pre-anthropogenic meteoric water, while samples with higher values (~ 2000 – $93,700 \times 10^{-15}$) indicate the input of anthropogenic meteoric fluid. Taking into account the geological, hydrologic and climatic features of the Atacama region, we propose that the mean contribution of anthropogenic ^{129}I is associated with ^{129}I releases during nuclear weapon tests carried out in the central Pacific Ocean until the mid 1990's ($^{129}\text{I}/\text{I} = \sim 12,000 \times 10^{-15}$). This source reflects rapid redistribution of this radioisotope on a global scale. Our results support the notion of a long-lived continental iodine cycle in the hyperarid margin of western South America, which is driven by local

* Corresponding author. Present address: Departamento de Ciencias de la Tierra, Universidad de Concepción, Casilla 160-C, Concepción, Chile. Tel.: +56 41 2203587. E-mail address: fernandaalvarez@udec.cl (F. Álvarez).

hydrological and climate conditions, and confirm that groundwater was a key agent for iodine remobilization and formation of the extensive iodine-rich soils of Atacama.

© 2016 Elsevier Ltd. All rights reserved.

1. Introduction

The global iodine budget and its distribution are dominated by the marine system (Muramatsu and Wedepohl, 1998). Iodine naturally exists in different oxidation states from iodide (I^-) to iodate (IO_3^-). Throughout most of the oceans, iodate predominates (Sillen, 1961). On the other hand, in surface waters up to 50% of the dissolved iodine may be present as iodide (Wong, 1991). In addition to iodate and iodide species, volatile organic iodine (e.g., CH_3I , C_2H_5I , CH_2I_2) are produced in pelagic and coastal oceanic waters by phytoplankton and seaweeds (e.g., Lovelock et al., 1973; Carpenter et al., 2000).

Iodine is a biophilic element, which is mostly concentrated in organic-rich material. For this reason, and because of its large ionic radius and high mobility, iodine is strongly depleted in continental environments, and therefore, elevated concentrations in rocks, soils and waters are rare. However, iodine mineral occurrences have been reported in hyper-arid desert environments. Among these, the Atacama Desert, located in the western margin of northern Chile, is the world's premier iodine production province, and hosts some of the highest iodine concentrations known in continental environments (Ericksen, 1981). In the Atacama region, iodine is mostly stored in nitrate-bearing soils and, to a lesser extent, in supergene Cu deposits and marine sedimentary rocks. Furthermore, natural waters also show anomalous concentrations, in particular ground waters, thermal springs and rainwater (Álvarez et al., 2015).

Recent studies have reported iodine concentration data and $^{129}I/I$ isotopic ratios in rocks, sediments and nitrate soils, pointing to an "old" organic-rich sedimentary source for iodine in these reservoirs (Reich et al., 2013; Pérez-Fodich et al., 2014; Álvarez et al., 2015). Deep and protracted groundwater flow is thought to have played an essential role not only in the remobilization and deposition of iodine in Atacama, but has also been tied to transport of other soluble species such as copper, chromium, sulfate and even nitrate (Cameron et al., 2010; Cameron and Leybourne, 2005; Palacios et al., 2005; Reich et al., 2008, 2009, 2013; Pérez-Fodich et al., 2014; Álvarez et al., 2015).

Although these studies have recognized that natural water was a key agent of iodine enrichment in Atacama, only a few data of iodine concentration in surface and groundwater are available. In a recent study, Álvarez et al. (2015) report iodine concentrations of ground waters, thermal springs and rainwater in the Antofagasta and Tarapacá regions. These concentrations vary from 0.5 μM to 48 μM , averaging $\sim 12 \mu M$ in groundwater and geothermal waters. The high iodine concentrations documented by Álvarez et al. (2015) are consistent with previous studies (e.g., Leybourne and Cameron, 2006) reporting similar concentrations ($\sim 50 \mu M$) in groundwater from the eastern of the Spence deposit. These data allow a preliminary assessment of iodine concentrations and distribution in natural waters in Atacama, and strongly suggest that iodine enrichment is more widespread than previously thought. However, the relative source contributions of iodine in the waters and its extent of mixing remain unknown. Furthermore, $^{129}I/I$ isotopic data in soil profiles reveal recent downward water flow that would shift the originally low $^{129}I/I$ ratios of caliche to higher, more meteoric values by isotopic mixing (Álvarez et al., 2015). Therefore, it is necessary to constrain the relative influence of pre-anthropogenic

iodine in natural waters, and the potential anthropogenic iodine inputs in Atacama. The estimated input from the major anthropogenic sources (e.g., nuclear tests, nuclear accidents and/nuclear fuel reprocessing) in the Atacama region, if present, remains unknown.

Here, we build on a previous study by Álvarez et al. (2015) and complement iodine data with major halogen (Br, Cl) concentrations in natural water samples from the Atacama region, including seawater, groundwater, rainwater, rivers, salt-lakes, and cold and thermal spring water. In addition, we constrain the $^{129}I/I$ isotopic signature of the waters and explore the environmental distribution of the ^{129}I radioisotope in northern Chile. By combining these data, we confirm that iodine is significantly enriched in most natural waters in Atacama, and its origin can be related to multiple natural and anthropogenic sources.

2. Background

2.1. Geological, climatic and hydrologic setting

The Atacama Desert is one of the driest environments on Earth and makes up much of the hyperarid margin of western South America (Fig. 1). It is located between the central Andes and the Pacific Ocean, in the western margin of northern Chile (18° – $26^\circ S$), where the Nazca Plate subducts beneath the South American Plate (Fig. 1). In the central Atacama region (20° – $25^\circ S$), five different morphostructural units are identified from west to east: (1) Coastal Cordillera, (2) Central Depression, (3) Precordillera, and (4) Western Cordillera, (5) Altiplano or Puna (Fig. 1). The Coastal Cordillera is mainly composed of Jurassic to lower Cretaceous intrusive and volcanic rocks of andesitic composition. In the north portion, its eastern border is composed of Jurassic marine back-arc sequences (Marinovic et al., 1995; Amilibia et al., 2008). The Central Depression is mainly covered by Neogene gravels with scattered outcrops of the Jurassic – Early Cretaceous marine/continental sediments and Cretaceous volcanic units occur. Sedimentary rocks include fluvial, lacustrine, playa, and nitrate deposits with interbedded volcanic ashes. The Precordillera is formed by Paleozoic to Mesozoic sedimentary and volcanic sequences, which were intruded by Paleozoic to Triassic and Paleocene-Eocene plutonic rocks (Hervé et al., 1991). The Western Cordillera is composed mostly of Tertiary andesitic volcanic rocks with minor outcrops of Paleozoic sedimentary and magmatic basement (Marinovic and García, 1999; Cortés, 2000; SERNAGEOMIN, 2003).

The current extreme hyperaridity of the Atacama Desert have been attributed to three major factors (e.g., Houston and Hartley, 2003): (1) subtropical atmospheric subsidence; (2) the coastal temperature inversion related to the upwelling caused by the cold Humboldt current, which prevents precipitation in the coastal regions; and (3) the rain-shadow effect caused by the high altitude of the Andean Cordillera, which prevents the progress of humid air masses from the Atlantic Ocean. The hyperarid core of the Atacama Desert receives less than 2 mm/yr, and occasional rainfalls occur only once every decade (Houston and Hartley, 2003; Garreaud et al., 2010). Despite the absence of precipitation, the western margin of the Atacama Desert receives consistent moisture in the form of coastal fog or sea spray from the Pacific Ocean, at elevations between 300 and 1000 m a.s.l. (Rundel et al., 1991). Occasional

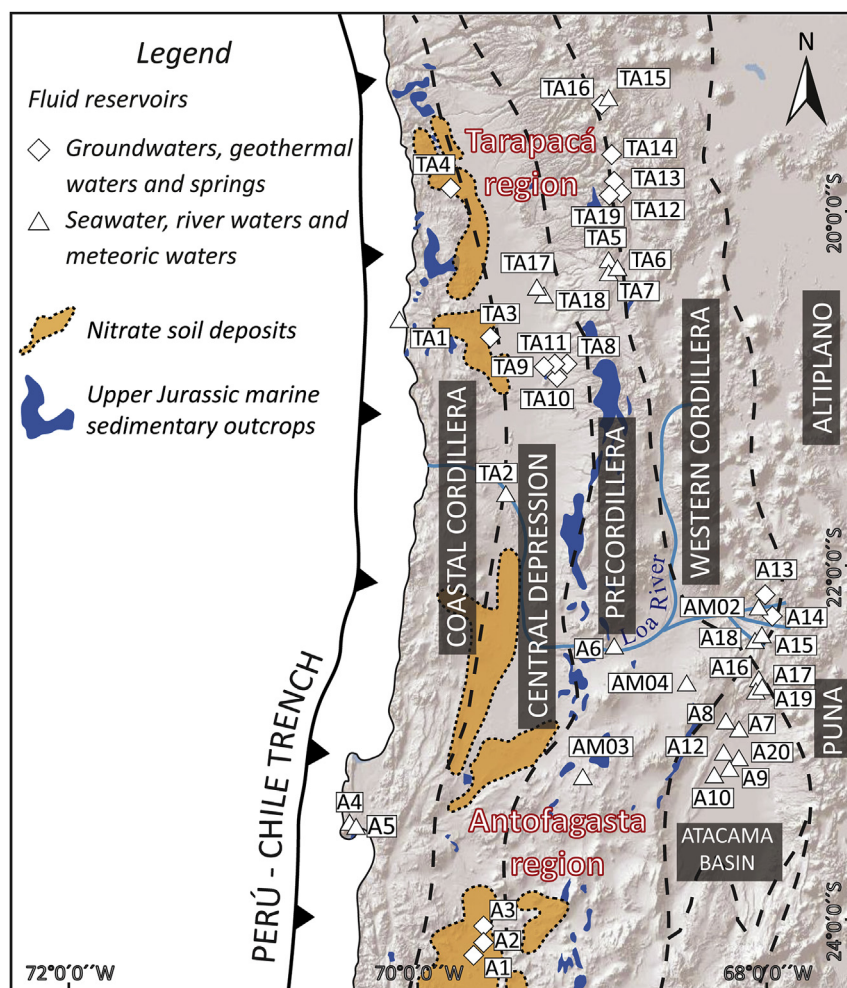


Fig. 1. Map of the studied area showing the main morphological units and the distribution of samples.

precipitation events in the central Atacama Desert generally result from Pacific air masses that migrate northward from the westerly precipitation well. Precipitation in the eastern margin of the Atacama Desert reaches 20 mm/yr at the base of the Andes (~2500 m), but this value increases strongly with the altitude. Precipitation is associated with the South American Summer Monsoon, causing rain fall between December and March (e.g., Aravena et al., 1999; Garreaud and Aceituno, 2001).

The precipitation pattern previously described is the main control of the hydrology in the region. Due to the extreme hyperaridity of the Atacama Desert, an almost exclusively endorheic drainage system has been developed. The only river in the study area with perennial stream flow is the Loa River, which flows from the Andes across the desert to the ocean (Fig. 1). Thus, the main source of water is precipitation in the High Andes (recharge areas), originating a base flow that goes from east to west (Magaritz et al., 1990; Aravena, 1995). Groundwater is frequently stored in aquifers of sedimentary origin, which were deposited during the Neogene and Quaternary (Magaritz et al., 1990). Discharge generally occurs as fracture flow through the volcanic units situated at the foothills of the Andes and through alluvial fans in *salar*s located at the terminus of the groundwater flow system in the Atacama Desert (Magaritz et al., 1990; Aravena et al., 1999).

2.2. Halogen geochemistry and the ^{129}I isotopic system

Elements from the halogen group are distributed distinctively in

the crustal reservoirs. While iodine is strongly related to organic matter, chlorine is mainly stored in seawater with a negligible biophilic behavior (Fabryka-Martin et al., 1991). The chemical behavior of bromine lies between iodine and chlorine; its major reservoir is seawater, but it is also related with organic material, although to a lesser degree than iodine. In fact, elevated bromine concentrations have been reported in pore fluids entrapped in organic-rich marine sediments (Martin et al., 1995).

Iodine has the most biophilic nature of the major halogens, and its geochemical behavior is considerably different from chlorine and bromine. Iodine has one stable isotope (^{127}I) and a long-lived radioisotope (^{129}I), with a half-life of 15.7 Ma. In nature, the radioisotope ^{129}I has two major production paths: a cosmogenic component, which is produced by cosmic ray-induced spallation of Xe isotopes in the atmosphere, and a fissiogenic component associated with spontaneous fission of ^{238}U in crustal rocks. Both mechanisms contribute similar amounts of natural ^{129}I to reservoirs in the earth's surface, particularly the ocean (Fabryka-Martin et al., 1985).

A potential inconvenience in the application of this isotopic system is the recent release of anthropogenic ^{129}I (Moran et al., 1999a; Snyder and Fehn, 2004). Since the onset of the nuclear age, the natural amount of ^{129}I and the isotopic equilibrium in surface reservoirs have been severely disturbed by the addition of anthropogenic iodine. Considering the residence time of iodine in the atmosphere (about 14 days; Rahn et al., 1976), all the surface reservoirs could present an anthropogenic signal, due to the

widespread dispersal of this element. Three major paths of released ^{129}I have been reported. A large quantity of ^{129}I was released from atmospheric bomb tests between 1945 and 1964 (Raisbeck et al., 1995; Wagner et al., 1996). Other input comes from nuclear accidents (e.g., Chernobyl, 1986; Fukushima, 2011). Finally, the more important source is ^{129}I released from fuel reprocessing plants, which has globally increased in five or more orders of magnitude the $^{129}\text{I}/\text{I}$ ratios (Moran et al., 1999a). However, this perturbation has not affected marine sediments or deep fluids (Moran et al., 1999b; Snyder and Fehn, 2004).

Thus, the iodine isotopic system has useful applications in geological systems, particularly in the age determination and tracing of fluids related to organic matter (e.g., marine sedimentary formations). For example, the measured iodine isotopic composition can be used to determine the iodine source, age of separation and pathways (e.g., Fehn et al., 2000; Snyder et al., 2003; Snyder and Fabryka-Martin, 2007). On the other hand, anthropogenic signal is useful to trace atmospheric and marine currents (e.g., Edmonds et al., 2001; Santschi et al., 2002; Yiou et al., 2002), study the transport of ^{129}I in rivers (e.g., Cochran et al., 2000; Moran et al., 2002; Snyder and Fehn, 2004) and determine the cumulative releases of short-lived radioisotopes produced during nuclear activity (e.g., Rao and Fehn, 1999; Reithmeier et al., 2010).

Due to the high mobility of iodine and its residence time in the seawater (300,000 yr; Broecker and Peng, 1982), which is much longer than the turnover time, the isotopic signal in all surface reservoirs connected with the ocean (e.g., oceans, shallow sediments, atmosphere, biosphere) is practically homogeneous. Therefore, a single, constant initial ratio is expected to be applicable to pre-bomb (anthropogenic) applications. The ^{129}I -to-stable ^{127}I isotopic ratio ($^{129}\text{I}/\text{I}$) has a constant value of 1500 ± 150 ($\times 10^{-15}$) at $\cdot \text{at}^{-1}$, and is used as the input value for ^{129}I calculations (Moran et al., 1998; Fehn et al., 2007a). Because of the presence of only one stable isotope of iodine (^{127}I) and the fact that the radiogenic isotope ^{129}I is present in very small amounts, $^{129}\text{I}/\text{I}$ (^{129}I over total iodine) is practically identical to $^{129}\text{I}/^{127}\text{I}$.

3. Methods

Water samples were collected in an area of $\sim 100,000$ square kilometers, including waters from the Pacific Ocean to the high Andes (Fig. 1). These samples are representative of the different iodine-bearing geochemical reservoirs in Atacama, and include: (1) seawater sampled near the coast of Iquique and Antofagasta (Pacific Ocean); (2) groundwater sampled from deep wells below nitrate deposits and salars in the Central Depression; (3) fresh water sampled from surface streams in the Central Depression and Western Cordillera; (4) cold and thermal spring water sampled in the Precordillera; (5) geothermal water sampled from boiling pools at Puchuldiza and El Tatio geothermal fields, both located in the Western Cordillera; and (6) rainwater in the High Andes, collected using custom-made collectors (Álvarez et al., 2015). Water samples retrieved from each sampling location were filtered (0.45 μm Millipore filter) and tested in-situ for temperature, conductivity and pH. At each location 250 ml of water were collected for concentration measurements and 1000 ml for isotopic determinations. Dissolved chlorine concentrations were determined by ion chromatography at the Department of Geology, Universidad de Chile in Santiago (5% error, 1 σ). The total iodine and bromine content was determined using inductively-coupled plasma mass spectrometry (3% error, 1 σ) at the Department of Chemistry, Gakushuin University in Tokyo. Water samples were diluted 200–5000 times and tetramethyl ammonium hydroxide (1%) and Na_2SO_3 (100 ppm) were added to avoid loss of iodine from the solution.

Extraction of iodine and preparation of silver iodide (AgI) targets

for accelerator mass spectrometry (AMS) determinations followed previously established methods (Fehn et al., 1992), i.e., extraction into carbon tetrachloride (CCl_4) followed by back extraction using sodium bisulfite (NaHSO_3) or hydroxylamine hydrochloride ($\text{NH}_2\text{OH}\cdot\text{HCl}$). Finally, approximately 1 mg of iodine was precipitated as AgI targets. The AMS measurements were performed at AMS Facility, University of Arizona, following established procedures (Sharma et al., 2000). Due to the small size of the targets, the results have larger margins than typical for AMS determinations (5–10%). Uncertainties in samples where carrier was added reflect errors in isotopic determinations of the carrier material as well as of the actual samples.

4. Results

Most of the iodine concentrations of water samples analyzed in this study are reported by Álvarez et al. (2015). We complement the published data with measurements of bromine and chlorine concentrations in the same samples, including 19 water samples from the Tarapacá region and 22 from the Antofagasta region. Also, we present the $^{129}\text{I}/\text{I}$ isotopic ratios for 21 samples. Results for concentrations, as well as for $^{129}\text{I}/\text{I}$ ratios, are listed in Table 1. Of a total of 41 samples, 3 correspond to seawater from the South Pacific Ocean, 7 are groundwater from the Central Depression, 8 are cold spring water from the Precordillera, 7 correspond to cold and thermal springs from the Western Cordillera (from El Tatio and Puchuldiza geothermal fields), 5 samples were taken from salt lakes, 8 samples were taken from rivers and lakes, and 3 samples correspond to rainwater in the Western Cordillera.

Iodine concentrations range between 0.35 μM and 26 μM in Tarapacá and between 0.25 μM and 48 μM in Antofagasta. The highest concentrations of iodine were measured in groundwater below nitrate deposits with values between 0.5 μM and 48 μM , averaging ~ 12 μM . These high iodine concentrations are followed by water samples from the Puchuldiza (~ 21 μM) and El Tatio (~ 7 μM) geothermal fields in the Western Cordillera. Spring waters from the Precordillera present values between ~ 1 and 12 μM (averaging ~ 5 μM). Finally, the lowest iodine contents were measured in seawater, surface waters and waters from salt lakes (“salars”) with concentrations from 0.25 to 8 μM , with an average of ~ 0.7 μM .

Chlorine concentrations of samples range from 0.61 mM to 69.2 mM in Tarapacá, and from 1.4 mM to 202.6 mM in the Antofagasta region (Table 1). Finally, bromine concentrations vary from 1.3 μM to 45.7 μM in Tarapacá and from 1.7 μM to 87.4 μM in Antofagasta. These ranges of values exclude water samples that have been exposed to high evaporation rates and samples with evidence of bedrock/evaporite dissolution. The measured halogen concentrations for meteoric water and seawater in the two regions present very similar values. Halogen concentrations in meteoric water shown averages of $\text{Cl} = 0.08$ mM, $\text{I} = 0.30$ μM and $\text{Br} = 0.44$ μM , while in seawater the average values are $\text{Cl} = 549$ mM, $\text{I} = 0.40$ μM and $\text{Br} = 610$ μM .

Concentrations of radiogenic iodine and $^{129}\text{I}/\text{I}$ isotopic ratio measurements in 12 water samples from Tarapacá and 9 samples from Antofagasta are reported in Table 1. Fig. 2 shows the isotopic ratios for each sample in Atacama. We identify two main groups. The first one includes the natural waters, which have $^{129}\text{I}/\text{I}$ ratios substantially above the pre-anthropogenic threshold value of 1500×10^{-15} (Fehn et al., 2007a), indicating the likely presence of anthropogenic ^{129}I . The isotopic ratios of these waters vary from ~ 1550 to $93,700 \times 10^{-15}$ (Table 1). There is a second group, where the natural waters have $^{129}\text{I}/\text{I}$ ratios lower than 1500×10^{-15} , which vary between ~ 215 and $\sim 1300 \times 10^{-15}$.

Table 1
Analytical results of halogen concentrations and $^{129}\text{I}/\text{I}$ ratios in water samples.

Sample	Type	Location		pH ⁺	T° (°C) ⁺	EC (μS/cm) ⁺	I(μM) ⁺	Br (μM)	Cl (mM)	$^{129}\text{I}/\text{I}$ ($10^{-15}\text{at}\cdot\text{at}^{-1}$)	1σ ($10^{-15}\text{at}\cdot\text{at}^{-1}$)	^{129}I ($10^7\text{at}/\text{L}$)
		Latitude (°S)	Longitude (°W)									
Tarapacá												
TA1	Seawater	20° 39' 36"	70° 11' 06"	8.1	17.2	ND	0.37	594.86	543.83	ND		
TA2	River	21° 37' 31"	69° 33' 17"	7.7	17.9	5870	1.56	19.76	ND	803.45	179.62	0.08
TA4	Groundwater	19° 53' 05"	69° 51' 54"	7.5	31.7	2780	7.25	8.18	11.84	9417.13	2319.71	4.11
TA5	Spring	20° 18' 23"	68° 52' 33"	6.1	14.5	ND	7.99	126.66	292.61	268.89	33.61	0.13
TA6	Salt lake	20° 18' 23"	68° 52' 33"	ND	ND	ND	1.00	5.72	8.80	ND		
TA7	Spring	20° 18' 32"	68° 52' 21"	6.7	15.6	940	0.35	3.98	7.68	ND		
TA8	Spring	20° 57' 50"	69° 10' 23"	7.3	22.1	2290	3.85	15.28	21.13	4742.53	911.62	1.10
TA9	Spring	20° 57' 50"	69° 10' 23"	7.4	22.1	2240	10.36	26.28	32.30	1551.97	334.48	0.97
TA10	Spring	20° 57' 50"	69° 10' 23"	7.3	21.8	2250	12.00	29.61	42.27	ND		
TA11	Spring	20° 55' 45"	69° 05' 48"	8.1	14.4	1950	3.76	13.91	18.69	14,461.37	2345.45	3.28
TA12*	Geothermal	19° 24' 38"	68° 58' 17"	8.4	19.2	3800	18.35	48.34	766.87	2148.90	947.14	2.37
TA13*	Geothermal	19° 24' 51"	68° 57' 45"	6.8	50.0	4300	15.23	44.14	725.17	4570.49	1299.96	4.19
TA14	Geothermal	19° 24' 44"	68° 57' 33"	8.0	84.0	4600	26.24	45.68	69.21	2851.72	1298.04	4.51
TA15	River	19° 40' 49"	69° 10' 53"	7.9	16.5	390	0.36	2.98	1.20	12,483.82	5021.79	0.27
TA16	Geothermal	19° 40' 59"	69° 10' 36"	8.4	40.0	450	0.54	1.89	1.53	ND		
TA17	Spring	20° 29' 14"	69° 19' 06"	8.2	30.3	170	1.25	1.28	0.61	1015.52	266.71	0.08
TA18	Spring	20° 29' 14"	69° 19' 06"	8.5	10.0	ND	2.29	2.26	1.65	ND		
TA19 ⁺⁺	Geothermal	19° 24' 30"	68° 57' 25"	8.1	33.0	ND	15.88	55.60	74.74	313.92	58.30	0.30
Antofagasta												
A1*	Groundwater	24° 10' 31"	69° 52' 07"	7.2	22.8	1570	48.12	20.02	3.22	217.00 ^{**}	15.00	0.63
A4	Seawater	23° 28' 10"	70° 30' 46"	7.8	16.8	ND	0.40	610.34	548.32	9982.27	2127.67	0.24
A5	Seawater	22° 28' 35"	68° 54' 51"	7.9	16.5	ND	0.44	623.15	554.74	11,971.56	2626.68	0.32
A6	River	22° 55' 20"	68° 09' 59"	7.8	15.3	7235	0.93	10.32	61.33	2728.54	720.19	0.15
A7	Groundwater	22° 53' 25"	68° 12' 50"	6.4	28.6	3670	2.64	14.91	26.35	ND		
A9*	Salt lake	23° 03' 32"	68° 12' 49"	7.8	16.0	ND	6.18	108.77	831.86	8471.03	1058.88	3.15
A10	Groundwater	23° 03' 32"	68° 12' 49"	ND	ND	ND	0.46	6.85	38.15	ND		
A12	Salt lake	23° 07' 40"	68° 14' 39"	7.0	23.5	ND	0.25	2.09	29.34	ND		
A13	Geothermal	22° 19' 48"	68° 00' 36"	6.8	81.0	ND	7.92	87.38	202.58	2081.52	429.20	0.99
A14	Geothermal	22° 24' 24"	68° 00' 41"	6.4	85.5	ND	6.29	60.18	145.32	ND		
A15	Lake	22° 25' 58"	68° 02' 57"	7.7	16.9	1020	0.51	2.61	3.86	ND		
A16	Spring	22° 43' 12"	68° 02' 37"	ND	ND	ND	1.78	8.40	1.43	ND		
A17	River	22° 46' 09"	68° 04' 07"	8.4	11.0	2240	1.49	9.89	20.16	ND		
A18	Lake	22° 25' 58"	68° 02' 57"	7.7	13.9	1360	0.37	1.88	3.80	ND		
A19	River	22° 46' 09"	68° 04' 07"	8.8	20.2	2120	1.51	8.30	15.90	ND		
A20*	Salt lake	23° 03' 54"	68° 12' 52"	8.2	19.7	ND	3.59	100.23	7262.06	1301.14	162.64	0.28
AM-02	Rainwater	22° 25' 59"	68° 02' 57"	7.7	ND	1180	0.36	0.44	2.99	93,721.56	1593.07	0.13

ND: Not determined.

+ pH, T°, EC and iodine concentration data from Álvarez et al. (2015).

* Sample has been exposed to high evaporation rates or shows evidence of bedrock/evaporite dissolution.

++ Sample reported in this study.

** $^{129}\text{I}/\text{I}$ ratio from sample A1 from Álvarez et al. (2015).

5. Discussion

5.1. Halogen concentrations

Most of the iodine concentrations reported here are elevated

when compared to natural iodine reservoirs (Álvarez et al., 2015). For example, rainwater in Atacama has a mean iodine concentration of $\sim 0.3\ \mu\text{M}$ (Table 1), which is one order of magnitude higher than typical values ($0.015\ \mu\text{M}$; Takaku et al., 1995; Moran et al., 1999a). Moreover, freshwater from Atacama show average iodine

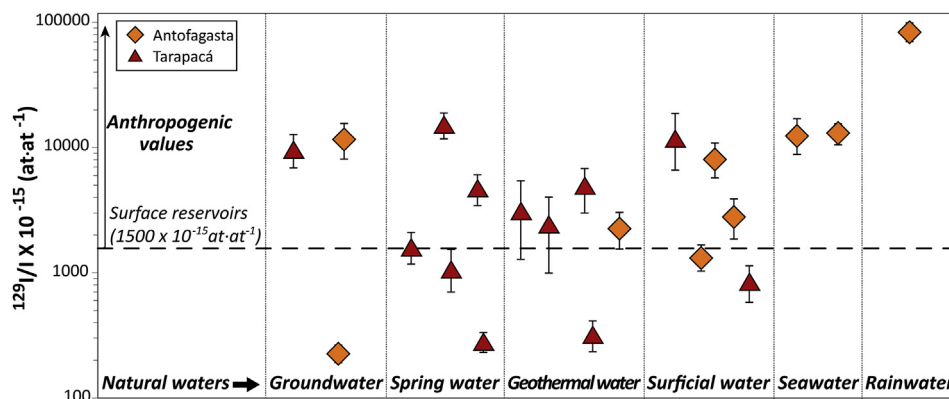


Fig. 2. Iodine isotopic ratios ($^{129}\text{I}/\text{I}$) of fluid samples from the Atacama Desert. Most of the $^{129}\text{I}/\text{I}$ ratios are above 1500×10^{-15} (initial isotopic ratio of surface reservoirs; Fehn et al., 2007a). Detailed information about water samples is presented in Table 1.

concentrations ($\sim 0.7 \mu\text{M}$, Table 1) of about one order of magnitude above the freshwater crustal average ($0.08 \mu\text{M}$, Muramatsu and Wedepohl, 1998), while groundwater samples are characterized by iodine concentrations within the same order of magnitude of fluids related to organic material (Fehn et al., 2007b). These high iodine concentrations are likely to be caused by the presence of an enriched source and/or due to the action of a subsequent concentration process (Pérez-Fodich et al., 2014; Álvarez et al., 2015). In order to identify which of these factors is predominant in the region, we use halogen correlation diagrams where chlorine concentrations are compared to iodine and bromine (Figs. 3 and 4). Water samples exposed to high evaporation rates and/or with evidence of dissolution of the bedrock were not considered for this analysis.

Chlorine, the most conservative halogen, is biophilically and petrologically incompatible (You and Gieskes, 2001). Lower chlorine concentrations in deep fluids (e.g., pore waters, deep groundwater) compared to higher values in seawater are explained by freshening due to water of meteoric and/or diagenetic origin (e.g. Kastner et al., 1991; Brown et al., 2001). Thus, chlorine preserves best the mixing behavior of the fluids between paleo-seawater and fresh water endmembers. Assuming that all the chlorine is of seawater origin (i.e., $\text{Cl} = 549 \text{ mM}$, Table 1) and was subsequently diluted by fresh water, initial iodine and bromine concentrations representatives of the primitive endmembers can then be estimated using regression lines in the halogen diagrams (Tomaru et al., 2007, 2009).

Iodine concentrations were plotted versus chlorine concentrations (Fig. 3), where two trends can be distinguished. These trends are distinctly different for each region; samples from Tarapacá follow the higher trend line, while samples from Antofagasta follow the lower trend line. Iodine concentrations of the initial fluids were estimated for each region resulting in two different endmembers with iodine concentrations of $\sim 150 \mu\text{M}$ in Tarapacá ($I/\text{Cl} = 0.34 \times 10^{-3}$) and $\sim 20 \mu\text{M}$ in Antofagasta ($I/\text{Cl} = 0.04 \times 10^{-3}$). These estimated values are much higher than that of seawater ($0.4 \mu\text{M}$ in the studied area; black star in Fig. 3), but are different in one order of magnitude between themselves. Due to the high iodine

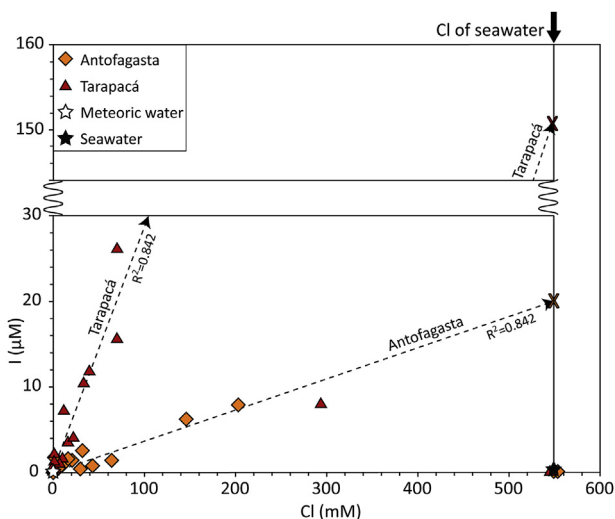


Fig. 3. Iodine vs. chlorine concentrations of fluids from the Atacama Desert. Segmented regression lines indicate mixing of meteoric water with enriched iodine fluids (one outlier sample from Tarapacá region was not considered for the regression). The “X” symbols at the right ends of these lines indicate the initial iodine concentration: $150 \mu\text{M}$ for Tarapacá fluids and $20 \mu\text{M}$ for Antofagasta fluids. Samples that have been exposed to high evaporation rates or with evidence of bedrock/evaporite dissolution were excluded of the analysis (Table 1).

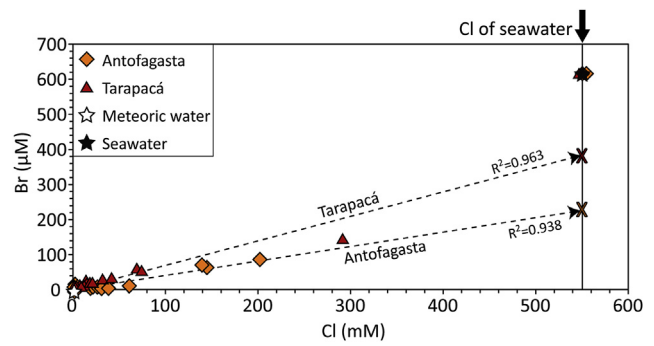


Fig. 4. Bromine vs. chlorine concentrations of fluids from the Atacama Desert. Segmented regression lines indicate mixing of meteoric water with enriched iodine fluids (one outlier sample from Tarapacá region was not considered for the regression). The “X” symbols at the right ends of these lines indicate the initial bromine concentration: $380 \mu\text{M}$ for Tarapacá fluids and $225 \mu\text{M}$ for Antofagasta fluids. Samples that have been exposed to high evaporation rates or with evidence of bedrock/evaporite dissolution were excluded of the analysis (Table 1).

concentration estimated for the initial fluids, our results confirm previous studies that these correspond to groundwater which has interacted with organic rich rocks and leached iodine (e.g., Pérez-Fodich et al., 2014; Álvarez et al., 2015). Furthermore, regression lines in Fig. 3 indicate mixing between the initial fluid and fresh water. In both cases, the extrapolation of each group of samples intersecting the x-axis ($I = 0 \mu\text{M}$) at $\text{Cl} = 0 \text{ mM}$ indicates that these fluids were more likely diluted by a low chlorine and, low iodine fluid, such as meteoric water (white star in Fig. 3), rather than seawater.

A similar diagram from bromine versus chlorine concentrations is shown in Fig. 4, but in this case no bromine enrichment is observed in Tarapacá or Antofagasta regions when compared to seawater. The diagram shows two different trends that represent mixing between the initial fluids and meteoric water (white star in Fig. 4). Similar to iodine, we back-calculated bromine concentrations of the initial fluids for Tarapacá and Antofagasta resulting at $\sim 380 \mu\text{M}$ ($\text{Br}/\text{Cl} = 0.41 \times 10^{-3}$) and $\sim 225 \mu\text{M}$ ($\text{Br}/\text{Cl} = 0.67 \times 10^{-3}$), respectively. Both values lie within the same order of magnitude indicating only slight differences between the two groups; also, the estimated Br values are lower than in seawater (black star in Fig. 4), and higher than in meteoric water. Low Br/Cl ratios are commonly interpreted as fluids that have encountered the dissolution of halite, due to halite incorporates little Br into its structure (Holser, 1970). The difference between Br and Cl distribution into halite decreases the Br/Cl ratio of brines during halite dissolution (e.g., Stueber and Walter, 1991; Stueber et al., 1992). Therefore the Br/Cl ratios indicate that natural waters from the Atacama Desert have been interacting with brines, where salt dissolution would have happened.

In Fig. 5, the comparison between I/Cl and Br/Cl ratios of water samples supports the notion that the observed variations between Tarapacá and Antofagasta are mainly associated with iodine concentrations. While the I/Cl ratios vary over more than three orders of magnitude between the two regions, Br/Cl ratios vary in two orders of magnitude (with the exception of one sample, Fig. 5). All the samples would indicate that seawater not correspond to an end member - the data trend plots almost orthogonal to the seawater-meteoric water mixing line (Fig. 5).

The highest I/Cl ratios occur in the samples from the Tarapacá region. This region, reflecting major iodine enrichment respect to samples from the Antofagasta difference suggests that iodine has a distinctive geochemical history when compared to chlorine and bromine. Because iodine has the strongest affinity to organic

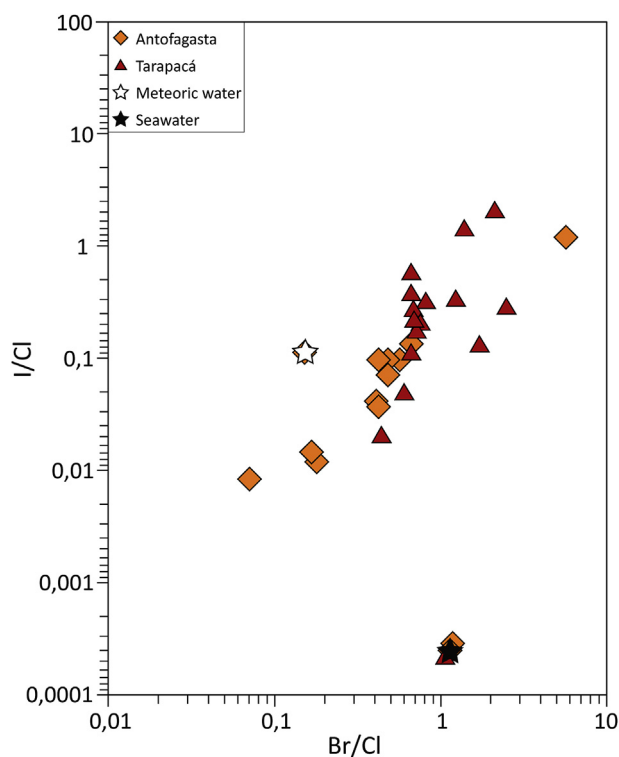


Fig. 5. I/Cl vs. Br/Cl diagram. Seawater (black star) and meteoric (rain) water (white star) are shown in the diagram.

material of the three halogens, the variation between the initial estimated concentrations probably reflects the existence of an organic-rich source. This is essential to obtain the current iodine enrichment in fluids from Atacama and without such a source concentration processes could not enriched preferentially iodine over bromine.

5.2. A pre-anthropogenic sources of ^{129}I

The evidence provided here is consistent with previous interpretations developed $^{129}\text{I}/\text{I}$ data in solid materials (rocks and soils), suggesting that the organic-rich source would be related to deep and old groundwater that has interacted with Jurassic marine sedimentary sequences over a protracted period (Reich et al., 2013; Pérez-Fodich et al., 2014; Álvarez et al., 2015). These sequences are the only sources with considerable amounts of organic content to explain the high levels of pre-anthropogenic iodine present in Atacama. However, we cannot rule out variable inputs of volcanic fluids into groundwater in the volcanic front (high Andes), as it has been previously proposed by Álvarez et al. (2015).

The low isotopic ratios reported in some natural waters from Atacama would indicate that these waters have no influence of a recent recharge, *i.e.*, the lower values reflect old waters without anthropogenic signature.

5.3. Anthropogenic sources of ^{129}I

The isotopic data for surface and ground water reported in this study provide additional insight into the more recent, anthropogenically-sourced iodine in the region. In Fig. 6, ^{129}I concentrations and $^{129}\text{I}/\text{I}$ isotopic ratios of water samples are plotted as a function of latitude. These values are compared to the global ^{129}I and $^{129}\text{I}/\text{I}$ data reported for shallow seawater (<3 m), river water,

lake water, snowmelt, and rainfall (data compiled by Snyder et al., 2010). In Atacama, all water samples have ^{129}I concentrations above the pre-anthropogenic limit, reaching values up to three orders of magnitude above this limit (Fig. 6A), while most of the $^{129}\text{I}/\text{I}$ isotopic ratios are higher than the pre-anthropogenic value of 1500×10^{-15} (Fig. 6B). Therefore, both ^{129}I concentrations and $^{129}\text{I}/\text{I}$ isotopic ratios reveal the existence of an anthropogenic signature in natural waters in Atacama.

Potential sources for anthropogenic (or post-nuclear era) iodine include nuclear weapon tests, where ^{129}I was released to the atmosphere during the main period of bomb testing (late 1940s to the 1960s; UNSCEAR, 2008). Some test sites potentially relevant to this study correspond to Novaya Zemlya in the Arctic Ocean (URSS), Bikini atoll (USA) and Mururoa atoll (France) in the central Pacific Ocean. An additional source of anthropogenic ^{129}I is related to nuclear fuel reprocessing plants. These are located in the Northern Hemisphere, where the reprocessing facilities at Sellafield (U.K.) and La Hague (France) are the main contributors to the European ^{129}I releases (Reithmeier et al., 2006). Finally, nuclear accidents such as the explosion of the Chernobyl reactor in 1986 (Michel et al., 2005) and the Fukushima accident in March 2011 have contributed significant amounts of ^{129}I to the atmosphere (Muramatsu et al., 2015).

Because of the virtual absence of any history of nearby releases from nuclear activity in South America, the ^{129}I concentrations and isotopic ratios measured in natural waters in Atacama are most likely related to inter-hemispheric transport and/or removal processes of anthropogenic iodine from nuclear tests, reprocessing of nuclear fuel and/or nuclear accidents. Although total iodine concentrations and $^{129}\text{I}/\text{I}$ data in natural waters are scarce in the Southern Hemisphere, some authors have investigated the anthropogenic signal of ^{129}I in surface reservoirs. Fehn and Snyder (2000) studied water samples mainly from Australia and New Zealand, suggesting that the most likely sources of anthropogenic ^{129}I correspond to releases from reprocessing plants located in the Northern Hemisphere. On the other hand, Reithmeier et al. (2010), based on model predictions and measured ^{129}I concentrations, proposed that the fallout from the atmospheric weapons tests is the dominant source of ^{129}I on the Southern Hemisphere, and suggested that the contribution to the present ^{129}I deposition fluxes by the gaseous releases from reprocessing facilities on the Northern Hemisphere is still very low. Recently, Negri et al. (2013) reported $^{129}\text{I}/\text{I}$ isotopic ratios in surface water and seawater samples from Argentina. The aforementioned authors also associate the measured ^{129}I values in Argentinian waters to levels related to nuclear weapon tests.

In the Atacama region, ^{129}I concentrations have values above nuclear testing, but below the modern average limit (Fig. 6A). Although the data presented here generally show ^{129}I concentrations lower than values measured in freshwater and shallow seawater from Europe, an important number of samples present roughly similar values to the ^{129}I concentrations reported in North America (Fig. 6A). In addition, it is noteworthy to mention that ^{129}I concentrations in Atacama are higher than values measured in rivers and lakes from Argentina (Negri et al., 2013), where the latter do not exceed the nuclear testing limit (Fig. 6A).

On the other hand, most of the $^{129}\text{I}/\text{I}$ ratios of water are above the pre-anthropogenic background, but unlike the ^{129}I concentrations, the isotopic ratios are below the nuclear testing limit and are significantly lower than isotopic ratios reported in the Northern Hemisphere (Fig. 6B) (e.g., Rucklidge et al., 1994; Rao and Fehn, 1999; Snyder et al., 2010). Moreover, $^{129}\text{I}/\text{I}$ ratios from Argentina (Negri et al., 2013) are slightly higher than values reported here. Therefore, a clear difference is observed between the ^{129}I concentrations and $^{129}\text{I}/\text{I}$ isotopic ratios when these values are compared

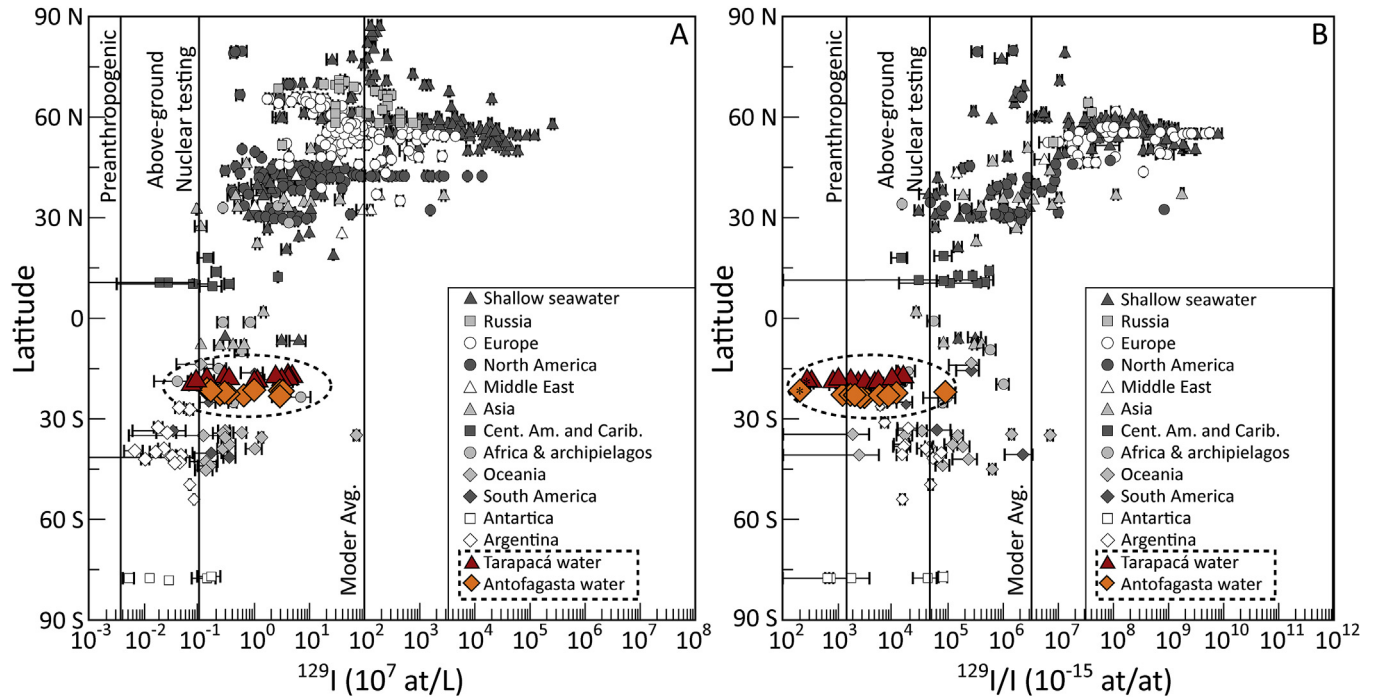


Fig. 6. (A) Concentrations of ^{129}I as a function of latitude show values in Tarapacá and Antofagasta are comparable with data from the Northern Hemisphere. (B) Ratios of $^{129}\text{I}/\text{I}$ indicate difference between the Northern Hemisphere and samples from Tarapacá and Antofagasta. Samples with (*) symbol correspond to deep waters with pre-anthropogenic $^{129}\text{I}/\text{I}$ ratios. Isotopic data were compiled by Snyder et al., 2010 and $^{129}\text{I}/\text{I}$ ratios from Argentina were reported by Negri et al., 2013.

to global iodine data.

We propose that the strong iodine enrichment of natural waters from Atacama is the cause of this difference. The high ^{129}I concentrations reported in Atacama (Fig. 6A) have been affected by the widespread regional iodine enrichment, reaching values within the same order of magnitude than in the Northern Hemisphere. However, when ^{129}I concentrations are normalized with respect to the local background (*i.e.*, total iodine concentration), the effect of iodine enrichment is suppressed. A comparison between Fig. 6A and B shows that all iodine global data but Atacama's remain approximately within the same ^{129}I anthropogenic origin range. Therefore, the radiogenic iodine distribution of natural waters from the Tarapacá and Antofagasta regions are indicative of the unique iodine enrichment in the Atacama Desert. According to this analysis, care must be taken in all future studies of natural and anthropogenic iodine tracing of water in the Atacama region, and $^{129}\text{I}/\text{I}$ isotopic ratios must be used rather than non-normalized ^{129}I concentrations.

Our data show that most of the $^{129}\text{I}/\text{I}$ ratios have similar levels to the values associated with nuclear tests (Fig. 6B), suggesting that the ^{129}I released to the atmosphere is present in natural waters from Atacama. The nearest sites where atmospheric and underground nuclear tests were carried out correspond to the Mururoa and Fangataufa atolls in French Polynesia, central Pacific Ocean. There were essentially two types of experiments carried out at Mururoa and Fangataufa: nuclear-weapon tests in which nuclear devices were exploded, and nuclear-weapon safety trials (IAEA, 1998). Most of the tests were conducted at Mururoa, the larger of the two atolls, and the rest, mostly the larger tests, were conducted at Fangataufa. Both the tests and the trials were conducted in the atmosphere as well as underground. There were 41 tests conducted in the atmosphere, 37 at Mururoa and four at Fangataufa, most of them by hanging the device from a balloon at a considerable elevation above the ground. There were 137 underground tests — 127 at Mururoa and ten at Fangataufa, the majority of which were

conducted with devices lowered into holes drilled into the rock beneath either the rim or the lagoon of the atolls. There were fifteen safety trials in all — five conducted in the atmosphere and ten underground (IAEA, 1998).

Given the geographical location of Mururoa and Fangataufa (equidistant from the east coast of Australia and the western coast of South America), it is likely that ^{129}I derived from nuclear testing in the Pacific would have been transported eastwards from the central Pacific to the South American margin through the prevailing westerlies winds developed at subtropical latitudes, where marine currents and wind patterns are responsible for the rapid redistribution of this radioisotope across the Pacific (*e.g.*, Garreaud, 2009).

Finally, we evaluate the Fukushima accident as an additional source of anthropogenic ^{129}I . However, our samples were collected before and after the nuclear accident, and they have no relation to the sampling date. Thus, this source is less feasible and will not be considered in the following discussion.

5.4. Relative contributions of pre-anthropogenic vs. anthropogenic sources for iodine in Atacama waters

Summarizing the previous discussions, the analysis of halogen concentrations in Atacama waters indicate that the main source of iodine in the region is groundwater which has interacted with organic rich rocks, which was preferentially diluted by meteoric water, most likely rainwater precipitated in the High Andes. Regarding isotopic data, the lower $^{129}\text{I}/\text{I}$ ratios (between ~ 215 and $\sim 1300 \times 10^{-15}$) are indicative a mixing between pre-anthropogenic meteoric waters and the ^{129}I anthropogenic free groundwater. On the other hand, the high isotopic ratios in water (between ~ 1550 and $93,700 \times 10^{-15}$) suggest an appreciable component of anthropogenic ^{129}I related to atmospheric source, presumably associated with nuclear bomb tests carried out in the central Pacific Ocean.

In order to determine the effect of atmospheric ^{129}I on isotopic

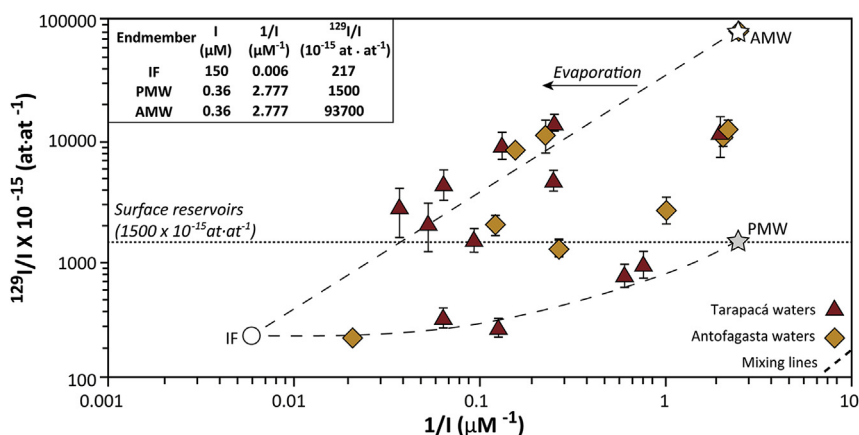


Fig. 7. $^{129}\text{I}/\text{I}$ ratios vs. reciprocal iodine concentrations. Mixing lines are indicated between the primitive endmember (initial fluid) and surficial endmembers: AMW (anthropogenic meteoric water) and PMW (pre-anthropogenic meteoric water).

ratios, as well as the effect of other potential (deeper) sources for iodine, we plotted the $^{129}\text{I}/\text{I}$ isotopic ratios versus the reciprocal of iodine concentration (Fig. 7). As a first approximation, we propose a fluid mixing model between the groundwater, the “initial fluid” (IF), which represent the highest estimated iodine concentration of the initial fluid found through I/Cl diagram (i.e., 150 μM) and the lowest isotopic ratio (217×10^{-15} , sample A1), and two surficial endmembers: (1) Anthropogenic meteoric water (AMW, white star in Fig. 7); and (2) Pre-anthropogenic meteoric water (PMW, grey star in Fig. 7). The composition of all endmembers is shown in the Fig. 7, where AMW corresponds to rainwater (sample AM02, Table 1), and the PMW endmember was defined with the pre-anthropogenic isotopic ratio of surface reservoirs (1500×10^{-15}) and the same measured iodine concentration in the sample AM02 (Table 1).

Most of the samples fall into the area bounded by IF-AMW and IF-PMW mixing lines, suggesting that observed isotopic ratios correspond to a mixing between the initial fluid and one or more surficial endmembers. Moreover, the samples with the lowest isotopic ratios (from 217 to 1015×10^{-15}) show a strong correlation with the IF-PMW mixing line, discarding the influence of an anthropogenically-contaminated source in the low $^{129}\text{I}/\text{I}$ ratio samples. Another group of samples are slightly shifted from the IF-AMW mixing line; we attribute this displacement to evaporation processes. Considering the absence of iodine isotopic fractionation during evaporation, it is possible to increase the total iodine concentration without affecting the isotopic ratios. Among these, previous works have been suggested significant evaporation of groundwater related to soil anomalies in the Central Depression (Leybourne and Cameron, 2006; Leybourne et al., 2013). Some samples that show this behavior correspond to thermal springs from Puchuldiza geothermal field. This site is located 4200 m above sea level, where extreme climatic conditions related to high evaporation rates occur (Nicolau et al., 2014).

Thus, mixing diagram analysis confirms the presence of two atmospheric iodine sources in the Atacama Desert. The way that iodine enters to Atacama is due to different transporting agents, which correspond to (1) wind patterns from the Pacific Ocean and (2) rainwater fall in the high Andes.

5.5. Hydrological cycling of iodine in Atacama

Based on the previous analysis, we propose a hydrological cycle model for iodine in Atacama, which allows explaining the high occurrence of iodine in natural waters (i.e., freshwater, rainwater

and groundwater). The proposed model (1) integrates “old” and recent additions of iodine with distinct isotopic signatures, (2) explains the widespread iodine enrichment observed in Atacama waters, and (3) is consistent with the climatic evolution and hydrology of the Atacama region (Fig. 8).

Precipitation in the High Andes is associated with the South American Summer Monsoon, where air masses spill over the central Andes and generate rainfalls at elevations above ~ 2800 m a.s.l. (Houston and Hartley, 2003). The Atlantic Ocean is the main source of precipitation in this zone. In this area evaporated waters from salt-lakes and thermal springs also contribute as a minor source of iodine in rainwater. These evaporated waters have variable inputs of meteoric and volcanic fluids.

Thus, the concentration and isotopic signature of iodine in rainwater in Atacama ($I = 0.29 \mu\text{M}$; $^{129}\text{I}/\text{I} = \sim 93,700 \times 10^{-15}$), reflect mixing between the local iodine reservoir and iodine sourced from the Atlantic Ocean.

On the other hand, the total iodine concentration in rainwater, which is one order of magnitude higher than the typical values (see section V.1), would reflect a process of local iodine enrichment. Considering the high evaporation rates reported in salt-lakes and thermal springs (Houston and Hartley, 2003; Nicolau et al., 2014), the most likely hypothesis is that this process could increase the available iodine in the atmosphere, promoting the subsequent pre-enrichment detected in rainwaters from Atacama.

The precipitation over the High Andes generates surface water runoff and infiltration to aquifers (Magaritz et al., 1990). Thus, iodine is transported westwards along with other chemical species by groundwater flow, which leach “old” iodine from sedimentary rocks located in the Precordillera (Pérez-Fodich et al., 2014; Álvarez et al., 2015). The isotopic signature of iodine stored in these sequences reflects both, an old component related to the Jurassic marine basin and a younger component associated with rainwater water fall in the high Andes.

Then, groundwater continues westwards to the Central Depression, where iodine precipitation is favored by an “impermeable” barrier effect at the eastern slope of the Coastal Cordillera.

The Atacama Desert also receives iodine inputs from the west. This component also reflects an anthropogenic signal related to anthropogenic ^{129}I that comes from nuclear weapon tests carried out in the central Pacific Ocean. This signature has elevated isotopic ratios (from ~ 2000 to $\sim 15,000 \times 10^{-15}$, Snyder et al., 2010, Fig. 6). Considering, the relatively short residence time of iodine in the atmosphere (about 14 days; Rahn et al., 1976), its mode of transport and high level of reactivity, the widespread dispersal of this

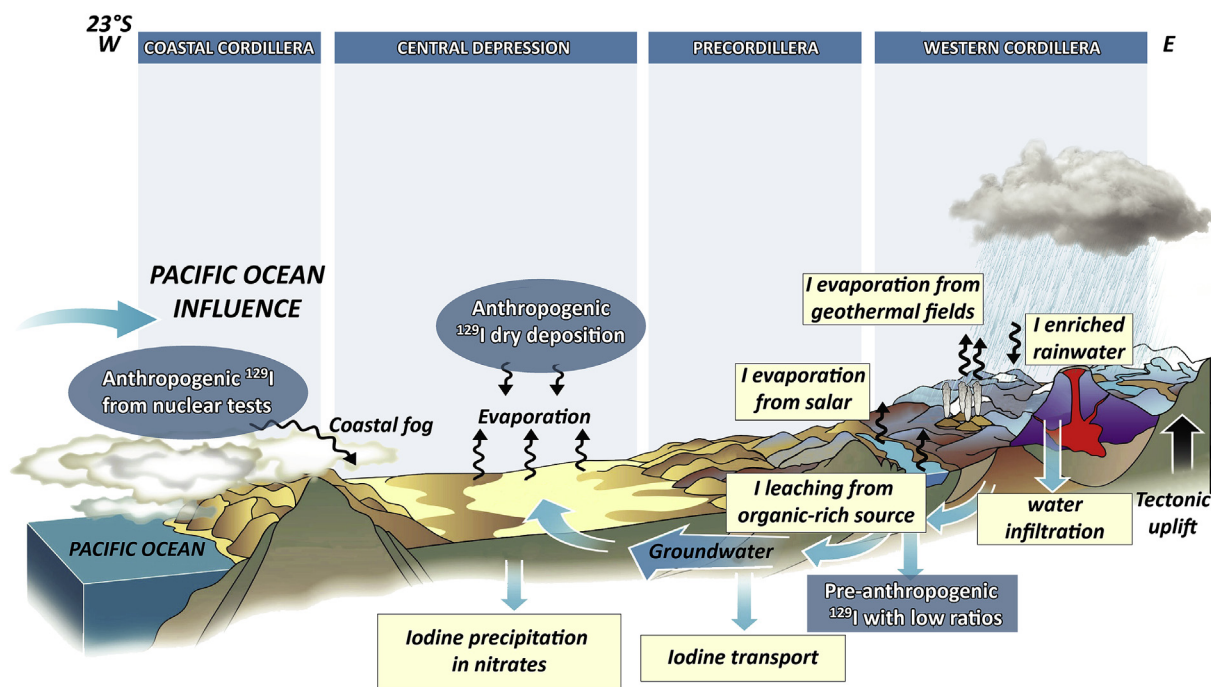


Fig. 8. Hydrological cycle of natural and anthropogenic iodine in the Atacama Desert.

element in surface waters is expected throughout the Atacama region.

6. Conclusion

This work presents the first comprehensive database of iodine isotope ratios in natural waters in Western South America. We show that natural waters in the Atacama Desert of northern Chile are enriched in iodine relative to mean crustal values, but not in the other halogens such as Cl or Br. In particular, the estimated iodine concentrations of the initial fluids in the Tarapacá and Antofagasta regions are three and two orders of magnitude, respectively, higher than those of seawater. Although I/Cl ratios in Tarapacá and Antofagasta are different in one order of magnitude, they are all derived from the same organic-rich source. Halogen diagrams also indicate dilution of the organic-rich fluid with meteoric water.

The $^{129}\text{I}/\text{I}$ ratios show influence of different natural and anthropogenic sources of iodine. Our results indicate that iodine in natural waters derives from one organic-rich (deep) source (i.e., marine Jurassic sequences and pore fluids in the Precordillera and Central Depression) and two atmospheric sources (pre-anthropogenic and anthropogenic meteoric water). Thus, we recognize an anthropogenically-contaminated source related to ^{129}I released during nuclear weapon tests carried out in the central Pacific Ocean. This source points to a rapid redistribution of this radioisotope on a global scale.

Acknowledgments

Financial support for this study was provided by FONDECYT grant 1100014 to Martin Reich. Additional support by MSI grant "Millennium Nucleus for Metal Tracing Along Subduction (NC130065) and FONDAP project 15090013 "Centro de Excelencia en Geotermia de los Andes, CEGA" is acknowledged. Fernanda Álvarez thanks CONICYT for providing support through a Ph.D. scholarship ("Programa de Becas de Doctorado"). We thank the

AMS group at PrimeLab, Purdue University and the AMS Facility at the University of Arizona for carrying out the ^{129}I measurements.

References

- Álvarez, A., Reich, M., Pérez-Fodich, A., Snyder, G.T., Muramatsu, Y., Vargas, G., Fehn, U., 2015. Sources, sinks and long-term cycling of iodine in the hyperarid Atacama continental margin. *Geochim. Cosmochim. Acta* 161, 20–70.
- Amilibia, A., Sàbat, F., McClay, K.R., Muñoz, J.A., Roca, E., Chong, G., 2008. The role of inherited tectono-sedimentary architecture in the development of the central Andean mountain belt: insights from the Cordillera de Domeyko. *J. Struct. Geol.* 30 (12), 1520–1539.
- Aravena, R., 1995. Isotope hydrology and geochemistry of northern Chile groundwaters. *Bull. Inst. Fr. Etudes Andin.* 24, 495–503.
- Aravena, R., Suzuki, O., Peña, H., Pollastri, A., Fuenzalida, H., Grilli, A., 1999. Isotopic composition and origin of the precipitation in northern Chile. *Appl. Geochem.* 14, 411–422.
- Broecker, W.S., Peng, T.H., 1982. *Tracers in the Sea*. Eldigio, Palisades, NY, p. 690.
- Brown, K.M., Saffer, D.M., Bekins, B.A., 2001. Smectite diagenesis, pore-water freshening, and fluid flow at the toe of the Nankai wedge. *Earth Planet. Sci. Lett.* 194, 97–109.
- Cameron, E.M., Leybourne, M.I., 2005. Relationship between groundwater chemistry and soil geochemical anomalies at the Spence copper porphyry deposit, Chile. *Geochem. Explor. Env.* 5, 135–145.
- Cameron, E.M., Leybourne, M.I., Reich, M., Palacios, C., 2010. Geochemical anomalies in northern Chile as a surface expression of the extended supergene metallogenesis of buried copper deposits. *Geochem. Explor. Env.* 10, 1–14.
- Carpenter, L.J., Malin, G., Liss, P.S., Küpper, F.C., 2000. Novel biogenic iodine-containing trihalomethanes and other short-lived halocarbons in the coastal East Atlantic. *Glob. Biogeochem. Cycles* 14, 1191–1204.
- Cochran, J.K., Moran, S.B., Fisher, N.S., Beasley, T.M., Kelley, J.M., 2000. Sources and transport of anthropogenic radionuclides in the Ob River system, Siberia. *Earth Planet. Sci. Lett.* 179, 125–137.
- Cortés, J., 2000. Hoja Palestina, Región de Antofagasta. Servicio Nacional de Geología y Minería. Mapas Geológicos, 19, 1 mapa escala 1:100.000. Santiago.
- Edmonds, H.N., Zhou, Z.Q., Raisbeck, G.M., Yiou, F., Kilius, L., Edmond, J.M., 2001. Distribution and behaviour of anthropogenic ^{129}I in water masses ventilating the North Atlantic Ocean. *J. Geophys. Res.* 106, 6881–6894.
- Erickson, G.E., 1981. *Geology and Origin of the Chilean Nitrate Deposits*. U.S. Geol. Surv. Prof. Paper 1188-B. United States Government Printing Office, Washington.
- Fabryka-Martin, J., Bentley, H., Elmore, D., y Airey, P.L., 1985. Natural I-129 as an environmental tracer. *Geochim. Cosmochim. Acta* 49, 337–347.
- Fabryka-Martin, J., Whittemore, D.O., Davis, S.N., Kubik, P.W., Sharma, P., 1991. Geochemistry of halogens in the Milk river aquifer, Alberta, Canada. *Appl. Geochem.* 6, 447.
- Fehn, U., Peters, E.K., Tullai-Fitzpatrick, S., Kubik, P.W., Sharma, P., Teng, R.T.D., Gove, H.E., Elmore, D., 1992. ^{129}I and ^{36}Cl concentrations in waters of the eastern

- Clear Lake area, California: residence times and source ages of hydrothermal fluids. *Geochim. Cosmochim. Acta* 56, 2069–2079.
- Fehn, U., Snyder, G., 2000. ^{129}I in the Southern Hemisphere: global redistribution of an anthropogenic isotope. *Nucl. Instr. Meth. Phys. Res.* 172, 366–371.
- Fehn, U., Snyder, G.T., Egeberg, P.K., 2000. Dating of pore waters with ^{129}I . Relevance for the origin of marine gas hydrates. *Science* 289, 2332–2335.
- Fehn, U., Moran, J.E., Snyder, G.T., Muramatsu, Y., 2007a. The initial $^{129}\text{I}/\text{I}$ ratio and the presence of “old” iodine in continental margins. *Nucl. Instrum. Meth. B* 259, 496–502.
- Fehn, U., Snyder, G.T., Muramatsu, Y., 2007b. Iodine as a tracer of organic material: ^{129}I results from gas hydrate systems and fore arc fluids. *J. Geochem. Explor.* 95, 66–80.
- Garreaud, R., Aceituno, P., 2001. Interannual rainfall variability over the South American Altiplano. *J. Clim.* 14, 2779–2789.
- Garreaud, R., 2009. The Andes climate and weather. *Adv. Geosci.* 22, 3–11.
- Garreaud, R., Molina, A., Farias, M., 2010. Andean uplift and Atacama hyperaridity: a climate modeling perspective. *Earth Planet. Sc. Lett.* 292, 39–50.
- Hervé, M., Marinovic, N., Mpodozis, C., Smoje, I., 1991. Mapa Geológico de la Hoja Sierra de Varas (1:100.000), Región de Antofagasta. Servicio Nacional de Geología y Minería. Documento de Trabajo 2.
- Holser, W.T., 1970. Bromide geochemistry of some non-marine salt deposits in the southern Great Basin. *Mineral. Soc. Am. Spec. Pap.* 3, 307–319.
- Houston, J., Hartley, A.J., 2003. The Central Andean west-slope rainshadow and its potential contribution to the origin of hyper-aridity in the Atacama Desert. *Int. J. Climatol.* 23, 1453–1464.
- IAEA, 1998. The Radiological Situation at the Atolls of Mururoa and Fangataufa. Technical Report. In: Releases to the Biosphere of Radionuclides from Underground Nuclear Weapons Tests, 4. International Atomic Energy Agency, Vienna.
- Kastner, M., Elderfield, H., Martin, J.B., 1991. Fluids in convergent margins: what do we know about their composition, origin, role in diagenesis and importance for oceanic chemical fluxes. *Philos. Trans. Roy. Soc. Lond.* 335, 243–259.
- Leybourne, M.I., Cameron, E.M., 2006. Composition of soils and ground waters at the Pampa del Tamarugal, Chile: anatomy of a fossil geochemical anomaly derived from a distant porphyry copper deposit. *Econ. Geol.* 101, 1569–1581.
- Leybourne, M.I., Cameron, E.M., Reich, M., Palacios, C., Faure, K., Johannesson, K.H., 2013. Stable isotopic composition of soil calcite (O, C) and gypsum (S) overlying Cu deposits in the Atacama Desert, Chile: implications for mineral exploration, salt sources, and paleoenvironmental reconstruction. *Appl. Geochem.* 29, 55–72.
- Lovelock, J.E., Maggs, R.J., Wade, R.J., 1973. Halogenated hydrocarbons in and over the Atlantic. *Nature* 241, 194–196.
- Magaritz, M., Aravena, R., Peña, H., Suzuki, O., Grilli, A., 1990. Source of ground water in the deserts of northern Chile: evidence of deep circulation of ground water from the Andes. *Ground Water* 28, 513–517.
- Marinovic, N., Smoje, I., Maksae, V., Hervé, M., Mpodozis, C., 1995. Hoja Aguas Blancas, Región de Antofagasta. Servicio Nacional de Geología y Minería, p. 150. Carta Geológica de Chile, No. 70.
- Marinovic, N., García, M., 1999. Hoja Pampa Unión, Región de Antofagasta. Servicio Nacional de Geología y Minería. Mapas Geológicos 9 (escala 1:100.000), Santiago.
- Martin, S., Ducker, R., Fort, M., 1995. A laboratory study of frost flower growth on the surface of young sea ice. *J. Geophys. Res.* 100, 7027–7036.
- Michel, R., Handl, J., Ernst, T., Botsch, W., Szidat, S., Schmidt, A., Jakob, D., Beltz, D., Romantschuk, L.D., Synal, H.A., Schnabel, C., López-Gutiérrez, J.M., 2005. Iodine-129 in soils from Northern Ukraine and the retrospective dosimetry of the iodine-131 exposure after the Chernobyl accident. *Sci. Total Environ.* 340, 35–55.
- Moran, J.E., Fehn, U., Teng, R.T.D., 1998. Variations in $^{129}\text{I}/^{127}\text{I}$ ratios in recent marine sediments: evidence for a fossil organic component. *Chem. Geol.* 152, 193–203.
- Moran, J.E., Oktay, S.D., Santschi, P.H., Schink, D.R., 1999a. Atmospheric dispersal of ^{129}I from European nuclear fuel reprocessing facilities. *Environ. Sci. Technol.* 33, 2536–2542.
- Moran, J.E., Oktay, S.D., Santschi, P.H., Schink, D.R., Fehn, U., Snyder, G., 1999b. World-wide Redistribution of ^{129}I from Nuclear Fuel Reprocessing Facilities: Results from Meteoric, River, and Seawater Tracer Studies. IAEA-SM-354/101.
- Moran, J.E., Oktay, S.D., Santschi, P.H., 2002. Sources of iodine and iodine in rivers. *Water Resour. Res.* 38, 1–9.
- Muramatsu, Y., Wedepohl, K.H., 1998. The distribution of iodine in the earth's crust. *Chem. Geol.* 147, 201–216.
- Muramatsu, Y., Matsuzaki, H., Toyama, C., Ohno, T., 2015. Analysis of ^{129}I in the soils of Fukushima prefecture: preliminary reconstruction of ^{131}I deposition related to the accident at Fukushima Daiichi nuclear power plant (FDNPP). *J. Environ. Radioact.* 139, 344–350.
- Negri, A., Fernandez, J., Wallner, A., Arazi, A., Fifield, L., Tims, S., 2013. ^{129}I Dispersion in Argentina: concentrations in fresh and marine water and deposition fluxes in Patagonia. *Environ. Sci. Technol.* 47, 9693–9698.
- Nicolau, C., Reich, M., Lynne, B., 2014. Physico-chemical and environmental controls on siliceous sinter formation at the high-altitude El Tatio geothermal field, Chile. *J. Volcanol. Geotherm. Res.* 282, 60–76.
- Palacios, C., Guerra, N., Townley, B., Lahsen, A., Parada, M., 2005. Copper geochemistry in salt from evaporite soils, coastal range of the Atacama Desert, northern Chile: an exploration tool for blind Cu deposits. *Geochim. Explor. Environ. Anal. A* 5, 371–378.
- Pérez-Fodich, A., Reich, M., Álvarez, F., Snyder, G.T., Schoenberg, R., Vargas, G., Muramatsu, Y., Fehn, U., 2014. Climate change and tectonic uplift triggered the formation of the Atacama Desert's giant nitrate deposits. *Geology* 42, 251–254.
- Rahn, K.A., Borys, R.D., Duce, R.A., 1976. Tropospheric halogen gases: inorganic and organic components. *Science* 192, 549–550.
- Raisbeck, G.M., Yiou, F., Zhou, Z.Q., Kilius, L.R., 1995. ^{129}I from nuclear fuel reprocessing facilities at Sellafield (UK) and La Hague (France): potential as an oceanographic tracer. *J. Mar. Syst.* 6, 561–570.
- Rao, U., Fehn, U., 1999. Sources and reservoirs of anthropogenic ^{129}I in western New York. *Geochim. Cosmochim. Acta* 63, 1927–1938.
- Reich, M., Palacios, C., Parada, M.A., Fehn, U., Cameron, E.M., Leybourne, M.I., Zúñiga, A., 2008. Atacamite formation by deep saline waters in copper deposits from the Atacama Desert, Chile: evidence from fluid inclusions, groundwater geochemistry, TEM, and ^{36}Cl data. *Min. Deposita* 43, 663–675.
- Reich, M., Palacios, C., Vargas, G., Luo, S., Cameron, E.M., Leybourne, M.I., Parada, M.A., Zúñiga, A., You, C.F., 2009. Supergene enrichment of copper deposits since the onset of modern hyperaridity in the Atacama Desert, Chile. *Min. Deposita* 44, 497–504.
- Reich, M., Snyder, G.T., Álvarez, F., Pérez, A., Palacios, C., Vargas, G., Cameron, E.M., Muramatsu, Y., Fehn, U., 2013. Using iodine isotopes to constrain supergene fluid sources in arid regions: insights from the Chuquicamata oxide blanket. *Econ. Geol.* 108, 163–171.
- Reithmeier, H., Lazarev, V., Rühm, W., Schwikowski, M., Gäggeler, H.W., Nolte, E., 2006. Estimate of European ^{129}I releases supported by ^{129}I analysis in an Alpine ice core. *Environ. Sci. Technol.* 40 (19), 5891–5896.
- Reithmeier, H., Lazarev, V., Rühm, W., Nolte, E., 2010. Anthropogenic ^{129}I in the atmosphere: overview over major sources, transport processes and deposition pattern. *Sci. Total Environ.* 408, 5052–5064.
- Rucklidge, J., Kilius, L., Fuge, R., 1994. ^{129}I in moss down-wind from the Sellafield nuclear reprocessing plant. *Nucl. Instr. Meth. Phys. Res.* 92, 417–420.
- Rundel, P.W., Dillon, M.O., Palma, B., Mooney, H.A., Gulmon, S.L., Ehleringer, J.R., 1991. The phytogeography and ecology of the coastal Atacama and Peruvian deserts. *ALISO* 13, 1–49.
- Santschi, P.H., Roberts, K.A., Guo, L.D., 2002. Organic nature of colloidal actinides transported in surface water environments. *Environ. Sci. Technol.* 36, 3711–3719.
- SERNAGEOMIN, 2003. Geologic Map of Chile, Digital Version, Scale 1:1000000.
- Sharma, P., Bourgeois, M., Elmore, D., Granger, D., Lipschutz, M.E., Ma, X., Miller, T., Mueller, K., Rickey, F., Simms, P., Vogt, S., 2000. PRIME lab AMS performance, upgrades and research applications. *Nucl. Instr. Meth. B* 172, 112–123.
- Sillen, L.G., 1961. The physical chemistry of seawater. In: Sears, M. (Ed.), *Oceanography*. Am. Assoc. Adv. Sci. Pub., Washington, DC, pp. 549–581.
- Snyder, G.T., Riese, R.C., Franks, S., Fehn, U., Pelzmann, W.L., Gorody, A.W., Moran, J.E., 2003. Origin and history of waters associated with coalbed methane: ^{129}I , ^{36}Cl , and stable isotope results from the Fruitland Formation, CO and NM. *Geochim. Cosmochim. Acta* 67, 4529–4544.
- Snyder, G.T., Fehn, U., 2004. Global distribution of ^{129}I in rivers and lakes: implications for iodine cycling in surface reservoirs. *Nucl. Instr. Meth. B* 223/224, 579–586.
- Snyder, G.T., Fabryka-Martin, J.T., 2007. ^{129}I and ^{36}Cl in dilute hydrocarbon waters: marine-cosmogenic, in situ, and anthropogenic sources. *Appl. Geochem.* 22, 692–714.
- Snyder, G., Aldahan, A., Possnert, G., 2010. Global distribution and long-term fate of anthropogenic ^{129}I in marine and surface water reservoirs. *Geochim. Geophys. Geosyst.* 11, 1–19.
- Stueber, A.M., Walter, L.M., 1991. Origin and chemical evolution of formation waters from Silurian-Devonian strata in the Illinois basin, USA. *Geochim. Cosmochim. Acta* 55, 309–325.
- Stueber, A.M., Walter, L.M., Huston, T.J., Pushkar, P., 1992. Formation waters from Mississippian-Pennsylvanian reservoirs, Illinois basin, USA: chemical and isotopic constraints on evolution and migration. *Geochim. Cosmochim. Acta* 57, 763–784.
- Takaku, Y., Shimamura, T., Masuda, K., Igarashi, Y., 1995. Iodine determination in natural and tap water using inductively coupled plasma mass spectrometry. *Anal. Sci.* 11, 823–827.
- Tomaru, H., Ohsawa, S., Amita, K., Lu, Z., Fehn, U., 2007. Influence of subduction zone settings on the origin of forearc fluids: halogen concentrations and $^{129}\text{I}/\text{I}$ ratios in waters from Kyushu, Japan. *Appl. Geochem.* 22, 676–691.
- Tomaru, H., Lu, Z., Fehn, U., Muramatsu, Y., 2009. Origin of hydrocarbons in the Green Tuff region of Japan: ^{129}I results from oil field brines and hot springs in the Akita and Niigata basins. *Chem. Geol.* 264, 221–231.
- UNSCEAR, United Nations Scientific Committee on the Effects of Atomic Radiation, 2008. Sources and Effects of Ionizing Radiation. Report to the General Assembly. United Nations, New York, USA.
- Wagner, M.J.M., Ditttrich-Hannen, B., Synal, H.A., Suter, M., Schotterer, U., 1996. Increase of ^{129}I in the environment. *Nucl. Instr. Meth. Phys. Res.* 113, 490–494.
- Wong, G.T.F., 1991. The marine geochemistry of iodine. *Rev. Aquat. Sci.* 4 (1), 45–73.
- Yiou, F., Raisbeck, G.M., Christensen, G.C., Holm, E., 2002. I-129/I-127, I-129/Cs-137 and I-129/Tc-99 in the Norwegian coastal current from 1980 to 1998. *J. Env. Radioact.* 60, 61–71.
- You, C.F., Gieskes, J.M., 2001. Hydrothermal alteration of hemi-pelagic sediments: experimental evaluation of geochemical processes in shallow subduction zones. *Appl. Geochem.* 16, 1055–1066.